The Journal of Chemical Physics

Dipole-bound and valence excited states of AuF anions via resonant photoelectron spectroscopy

Cite as: J. Chem. Phys. **154**, 074303 (2021); https://doi.org/10.1063/5.0038560
Submitted: 23 November 2020 . Accepted: 21 January 2021 . Published Online: 17 February 2021

Yuzhu Lu, Rulin Tang, Xiaoxi Fu, Hongtao Liu, and Chuangang Ning

The Journal of Chemical Physics ARTICLE scitation.org/journal/jcp

Dipole-bound and valence excited states of AuF anions via resonant photoelectron spectroscopy

Cite as: J. Chem. Phys. 154, 074303 (2021); doi: 10.1063/5.0038560
Submitted: 23 November 2020 • Accepted: 21 January 2021 •
Published Online: 17 February 2021

Yuzhu Lu,[1] Rulin Tang,[1] Xiaoxi Fu,[1] Hongtao Liu,[2] and Chuangang Ning[1,3,a)]

AFFILIATIONS

[1] Department of Physics, State Key Laboratory of Low Dimensional Quantum Physics, Tsinghua University, Beijing 10084, China
[2] Key Laboratory of Interfacial Physics and Technology, Shanghai Institute of Applied Physics, Chinese Academy of Sciences, Shanghai 201800, China
[3] Collaborative Innovation Center of Quantum Matter, Beijing 100084, China

[a)] **Author to whom correspondence should be addressed:** ningcg@tsinghua.edu.cn

ABSTRACT

Gold fluoride is a very unique species. In this work, we reported the resonant photodetachment spectra of cryogenically cooled AuF^- via the slow-electron velocity-map imaging method. We determined the electron affinity of AuF to be 17 976(8) cm^{-1} or 2.2287(10) eV. We observed a dipole-bound state with a binding energy of 24(8) cm^{-1}, a valence excited state with a binding energy of 1222(11) cm^{-1}, and a resonant state with an energy of 814(12) cm^{-1} above the photodetachment threshold. An unusual vibrational transition with $\Delta n = -3$ was observed in the autodetachment from the dipole-bound state. Moreover, two excited states of neutral AuF were recognized for the first time, located at 13 720(78) cm^{-1} and 16 188(44) cm^{-1} above the AuF ground state.

I. INTRODUCTION

Gold fluoride is very unique compared to its congeneric compounds MX (M = Cu, Ag, Au and X = F, Cl, Br, I). For example, the number of gold-fluoro compounds known today is still very small in contrast to the vast number of gold compounds containing chlorine, bromine, and iodine.[1] It was not until 1994 that AuF was unambiguously identified in the gas phase by Schwarz and co-workers.[2] In 1992, Saenger and Sun observed yellow emission bands, which were very likely from AuF.[3] Some vibrational structures were not resolved due to the limited resolution. An informative experiment by Butler *et al.*[4] presented accurate molecular constants of the ground and three excited states of AuF. For the ground state, they reported the vibration frequency ω_e = 563.609 04(19) cm^{-1} and the anharmonicity $\omega_e\chi_e$ = 2.896 284(63) cm^{-1}. The dipole moment of AuF ground state $X^1\Sigma^+$ is 4.13(2) D according to the Stark study of Steimle *et al.*,[5] which is large enough (>2.5 D) to possess a dipole-bound state (DBS).[6–11] Thus, it is expected that a DBS can be observed in the high-resolution photoelectron spectroscopy of AuF^-. There are many theoretic investigations of neutral AuF.[12–21] For example, the work of Guichemerre *et al.*[19] made extensive predictions of both ground and excited states of AuF. Recently, the photoelectron spectroscopy of CuF^- and AgF^- has been reported by the Mabbs group.[22,23] The electronic structures of CuF^- and AgF^- are relatively simple. Both CuF^- and AgF^- have a ground state and a DBS. Above the threshold, some resonance states were observed for both CuF^- and AgF^-, most of which were described as dipole-stabilized shape resonances.[23] In this work, we report the resonant photoelectron spectroscopy of a cryogenically cooled AuF anion using the slow-electron velocity-map imaging (SEVI) method.[24–28] To the best of our knowledge, no research of AuF^- has been reported.

II. EXPERIMENT SETUP

The experiment was carried out on our SEVI apparatus equipped with a cryogenically controlled ion trap.[29,30] Our recent

modifications have enabled us to switch between the SEVI mode and the scan mode so that we can acquire the photoelectron energy spectra in the SEVI mode and observe resonance peaks by scanning the wavelength of the photodetachment laser in the scan mode. The AuF^- anions were generated by laser ablation of a gold metal disk in the presence of NF_3 gas. The NF_3 gas was delivered onto the gold target before each ablation laser shot via a pulse valve. The time sequence was optimized to obtain the best AuF^- yield. The anions were captured by an octupole radio-frequency (RF) ion trap and cooled through collisions with the buffer gas (20% H_2 and 80% He). The ion trap was mounted on the second stage of a liquid helium refrigerator with a tunable temperature in the range of 5 K–300 K.[30–32] Then, the anions were ejected out by the pulsed potentials on the end caps of the trap and analyzed using a Wiley–McLaren type time-of-flight (TOF) mass spectrometer.[33] Strong signals of Au^-, AuF^-, and AuF_2^- were observed, and AuF^- was selected via a mass gate. The selected anions were then photodetached with a tunable laser, which crossed the ion beam perpendicularly. In the SEVI mode, the photoelectrons were projected onto a phosphor screen behind a set of microchannel plates and recorded by a charge-coupled device (CCD) camera. The maximum entropy Legendre expanded image reconstruction (MELEXIR) method[34] was used to reconstruct the 3D photoelectron distribution from the projected images. In the scan mode, electrons and anions were detected by the phosphor screen and recorded using a high-speed oscilloscope.[35] To obtain the photodetachment spectra of AuF^-, the signal light of an optical parametrical oscillator (OPO, 405 nm–709 nm for the signal light, and linewidth ~5 cm^{-1}) pumped by a Quanta-Ray Lab 190 Nd:YAG laser was used. 100 laser shots were collected for each data point. A tunable dye laser (400 nm–920 nm and linewidth 0.06 cm^{-1} at 625 nm) pumped by a Quanta-Ray Pro 290 Nd:YAG laser (20 Hz and 1000 mJ/pulse at 1064 nm) was employed to measure the electron affinity and investigate the rotational profiles of resonant peaks. The wavelength of the dye laser was measured by a wavelength meter (HighFinesse WS6-600, 0.02 cm^{-1} accuracy). This wavelength meter can also monitor the intensity of each laser pulse.

III. RESULTS AND DISCUSSION

Figure 1 shows the photoelectron spectra accumulated using the signal light of OPO at room temperature and 15 K. The spectra of Au^- were used for the energy calibration. It can be seen that hot bands, i.e., the peaks labeled as $1' \rightarrow 0$, $1' \rightarrow 1$, and $2' \rightarrow 0$, disappeared as the temperature dropped from 300 K to 15 K. These peaks were contributed by the vibrational exited states of AuF^- at its electronic ground state $X^2\Sigma^+$. The number with a prime indicated the vibrational quantum number of AuF^- at the $X^2\Sigma^+$ state. The vibrational frequency of AuF^- at its electronic ground state $X^2\Sigma^+$ was determined to be 405(99) cm^{-1}. To measure the electron affinity of AuF with higher accuracy, the photoelectron spectra were then collected at a photon energy of 18 000.56 cm^{-1}, just above the photodetachment threshold. As a result, the electron affinity of AuF was determined to be 17 976(8) cm^{-1} or 2.2287(10) eV. The uncertainty is mainly due to the rotational broadening. To observe the DBS in AuF^-, we scanned the photon energy from 16 000 cm^{-1} to 20 900 cm^{-1} and recorded the intensity of photoelectron signals at

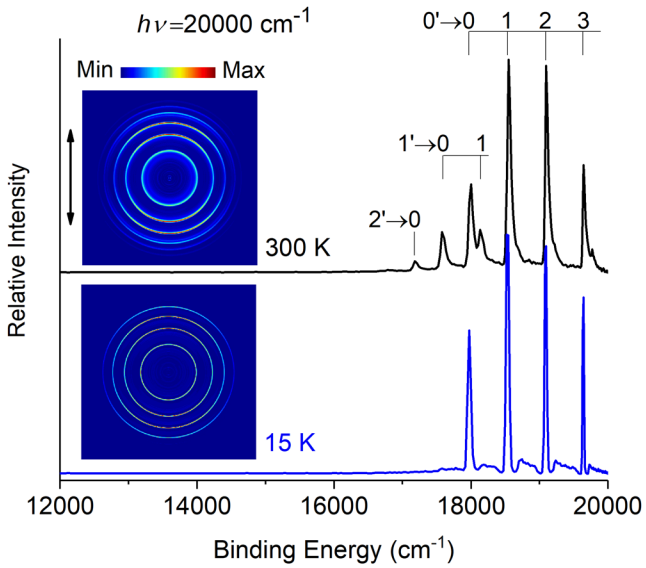

FIG. 1. Photoelectron images and spectra of AuF^- at 300 K (black line) and 15 K (blue line). The double arrow indicates the polarization of the detachment laser. The vibrational transitions are marked on the top.

15 K. Figure 2 shows the observed resonant structures. The peaks below the photodetachment threshold were contributed by resonant two-photon detachment (R2PD). Clearly, we observed two sets of resonances. The peaks labeled as v0 to v5 are almost evenly spaced, and peaks labeled as d0 to d4 form another nearly equi-spaced set.

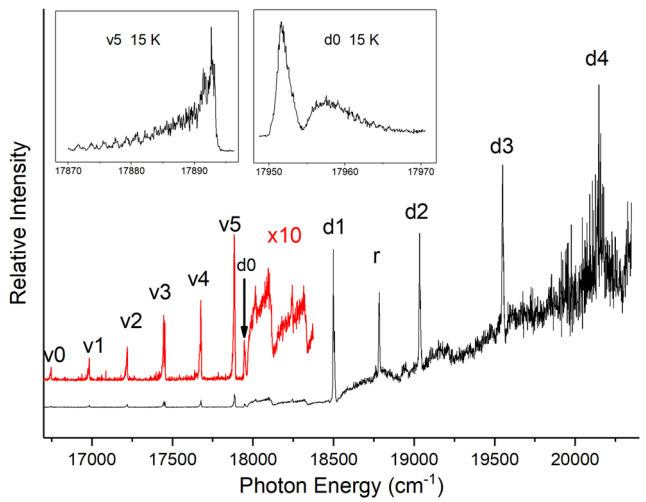

FIG. 2. Photodetachment spectrum of cryogenically cooled AuF anions by measuring the total electron yields as a function of the laser photon energy across the detachment threshold using the OPO signal light. The curve in red shows the weak peaks multiplied by a factor of 10. The insets show the rotational profiles of resonant peaks v5 and d0 using a dye laser with a narrow linewidth.

The two sets were assigned as the vibrational progressions related to two exited states of AuF^-. One is a valence excited state (VES) and the other is a DBS. Peak *r*, lying 814(12) cm^{-1} above the photodetachment threshold, is a resonance related to a different state. Peak v0 was assigned to be the vibrational ground state of the VES since no more vibrational peaks were observed when the photon energy was scanned further down. The vibrational frequency of the VES was determined to be 237(8) cm^{-1}. The vibrational frequency of the dipole bound state was determined to be 562(8) cm^{-1}, which is very close to the vibrational frequency 560.712 76(20) cm^{-1} of the ground state of neutral AuF.[4] Another evidence for the peak assignment is the rotational profiles of the resonant peaks. As shown in the insets of Fig. 2, the rotational profile of v5 is remarkably different from that of d0, which reflects the different Au–F bond lengths between the two states. The rotational profiles were recorded using our dye laser with a narrow linewidth 0.06 cm^{-1}. The energy levels of two excited states were determined to be 16 754(8) cm^{-1} (VES) and 17 952(2) cm^{-1} (DBS) above the AuF^- ground state, respectively. Therefore, the binding energy of the DBS was determined to be 24(8) cm^{-1} and 1222(11) cm^{-1} for the VES.

To interpret the observed spectra, we conducted multi-reference configuration interaction (MRCI) calculations using the Molpro software package.[36] The spin–orbit coupling has been included in the calculations. The correlation consistent basis sets aug-cc-pV5Z-PP for Au with ECP60MDF pseudopotentials[37] and aug-cc-pV5Z for F were used.[38] The calculations predicted two excited states below the neutral ground state, lying 1.9 eV ($2\ ^2\Sigma^+$) and 2.0 eV ($1\ ^2\Pi_{3/2}$) above the AuF^- ground state ($X^2\Sigma^+$). Higher states, located 2.4 eV ($1\ ^2\Delta_{5/2}$) and 3.2 eV ($1\ ^2\Pi_{1/2}$) above the anionic ground state, were also predicted, which were too high to be responsible for the observed valence excited state. The ground state $X^2\Sigma^+$ has a dissociation asymptote of $Au(^2S_{1/2}) + F^-(^1S_0)$. The excited states $2\ ^2\Sigma^+$ and $1\ ^2\Pi_{3/2}$ correspond to the $Au^-(^1S_0) + F(^2P_{3/2})$ asymptote. The calculated excited states $2\ ^2\Sigma^+$ and $1\ ^2\Pi_{3/2}$ might be responsible for the observed VES and the resonance state related to peak *r*, respectively. Guichemerre and co-workers did not include spin–orbit couplings in their calculations of the potential energy curves of neutral AuF.[19] Therefore, we calculated the potential energy curves for the ground and excited states of neutral AuF considering spin–orbit couplings. In Fig. 3, the potential energy curves of the related AuF^- and AuF states were plotted together. The curves of AuF^- DBS, AuF^- VES, and AuF^- $X^2\Sigma^+$ were generated using Morse potentials with the experimentally determined parameters, while the curves for neutral AuF were calculated using the method mentioned above.

Since the molecular parameters of neutral AuF have been experimentally determined with high accuracy, the dissociation energy $D_e(AuF, X^1\Sigma^+)$ was estimated to be 3.40 eV using the equation $D_e = \hbar\omega_e/4\chi_e$.[39] Then, with EA(AuF) = 2.2287(10) eV determined in the present work and EA(F) = 3.401 1895(25) eV as measured by Blondel *et al.*,[40] the dissociation energy of AuF^- can be given by $D_e(AuF^-, X^2\Sigma^+) = D_e(AuF, X^1\Sigma^+) + EA(AuF) - EA(F)$ = 2.23 eV, which is above the observed AuF^- excited states and very close to *EA*(AuF). Okabayashi *et al.*[41] also gave an estimation of $D_e(AuF, X^2\Sigma^+)$ = 3.01 eV using the molecular constants by fitting the pure rotational spectrum to the Dunham expression. The corresponding $D_e(AuF^-, X^2\Sigma^+)$ = 1.84 eV is below the energy level of AuF^- excited states. In addition, based on the reactions producing

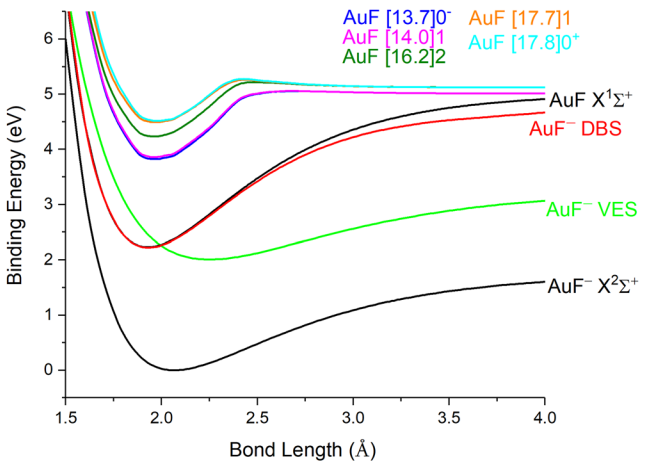

FIG. 3. Potential energy curves of the related AuF^- and AuF states. The curves of AuF^- DBS, AuF^- VES, and AuF^- $X^2\Sigma^+$ are generated using Morse potentials with the experimentally determined parameters, while the curves for the neutral AuF are the calculated results.

neutral AuF, Schröder *et al.*[2] estimated that the lower bound for $D_e(AuF, X^2\Sigma^+)$ was 3.16 eV and the upper bound was 3.69 eV, which set the bound for $D_e(AuF^-, X^2\Sigma^+)$ as [1.99 eV, 2.52 eV]. The resonant energies of peaks v0–v5 are in the range [1.99 eV, 2.52 eV]. Therefore, it is likely that some of the vibrational excited AuF^- VES are predissociated states. This can explain why the photoelectron yield in the range of 18 000 cm^{-1}–18 400 cm^{-1} unexpectedly reduced. If no predissociation occurs, the resonant peaks v6 and v7 are expected to be observed in this range. It should be pointed out that the features in the range of 18 000 cm^{-1}–18 400 cm^{-1} are not likely due to the signal fluctuation since we scanned the region for several times and the spectra showed the same features. A reasonable explanation is that AuF^- anions were quickly dissociated into Au and F^- and F^- cannot be photodetached by the laser due to the very high electron affinity of F atom.

The R2PD photoelectron spectra of v5 (VES) and d0 (DBS) are shown in Fig. 4. The spectra are due to the photodetachment from AuF^- $X^2\Sigma^+$ to the ground state and the excited states of neutral AuF via the intermediated states of AuF^-. The AuF excited states [14.0]1, [17.7]1, and $[17.8]0^+$ observed by Butler *et al.*[4] were recognized in the present work. Besides, two more states $[13.7]0^-$ and [16.2]2 were identified, and they are 13 720(78) cm^{-1} and 16 188(44) cm^{-1} above the AuF ground state $X^1\Sigma^+$, respectively. The states are labeled in Hund's case (c) notion $[T_0]\Omega$, where T_0 is the energy relative to AuF $X^1\Sigma^+$ in 1000 cm^{-1} and Ω is the total electronic angular momentum about the internuclear axis. The states $[13.7]0^-$ and [16.2]2 were predicted by the calculations of Guichemerre *et al.*[19] However, they were not observed by Butler *et al.*[4] in their search from 553 nm to 800 nm using laser excitation spectroscopy.

Figure 5 shows R2PD photoelectron spectra of v1–v5 in comparison with the Franck–Condon simulations. The R2PD photoelectron spectrum of v0 is not shown due to the very low signal-to-noise ratio. The Franck–Condon factors were calculated via the

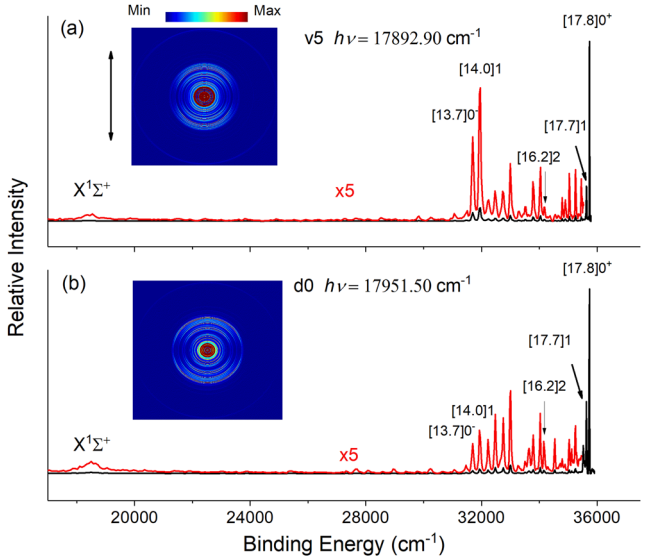

FIG. 4. Resonant two-photon photoelectron spectra and images of AuF^- via the valence excited state with the vibration quantum equal to 5 labeled as v5 (a) and the vibrational ground state of the dipole bound state labeled as d0 (b) using the dye laser. The red curves show the weak peaks multiplied by a factor of 5. The excited states of neutral AuF are labeled in Hund's case (c) notion $[T_0]\Omega$, where T_0 is the energy relative to AuF $X^1\Sigma^+$ in 1000 cm^{-1} and Ω is the total electronic angular momentum about the internuclear axis.

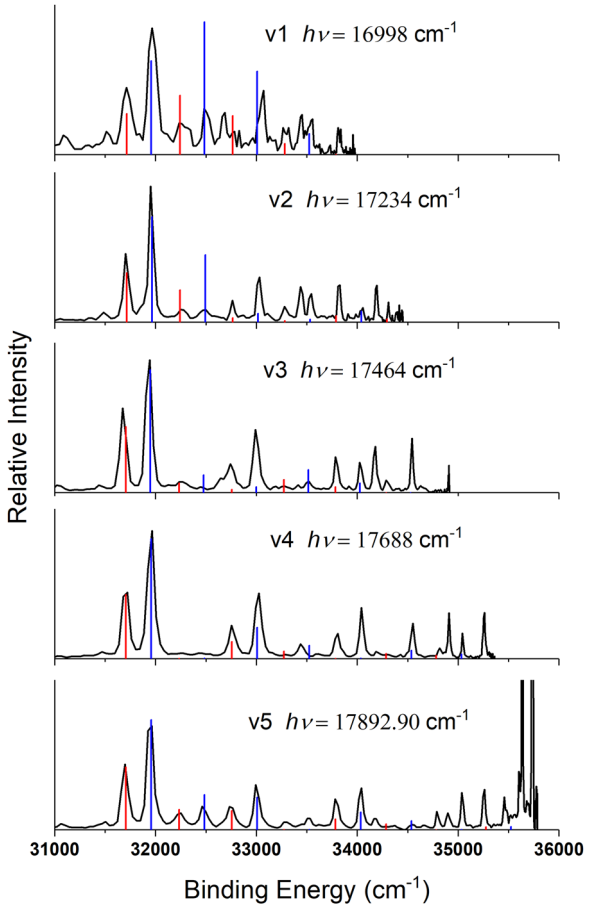

FIG. 5. Resonant two-photon photoelectron spectra of AuF^- via the valence excited state with vibrational quantum numbers equal to 1, 2, 3, 4, and 5 and Franck–Condon simulations. The bars in red denote the Franck–Condon progression corresponding to the AuF $[13.7]0^-$ state and the bars in blue denote the Franck–Condon progression corresponding to the AuF [14.0]1 state.

Morse potential using the method of López *et al.*,[42] and the bond length of AuF^- VES was optimized to be 2.16 Å. As shown in Fig. 5, the Franck–Condon simulation can roughly reproduce the major features of R2PD photoelectron spectra. However, significant discrepancies exist between the simulations and experimental results. The possible reasons for the discrepancies are as follows: the excited states of AuF^- are likely to be predissociated, so the vibrational wavefunction deviates considerably from that of the Morse potential, and the potential energy curves of excited states of neutral AuF also deviate significantly from the Morse potential due to the strong spin–orbit couplings, as illustrated in Fig. 3.

Figure 6 shows the resonance-enhanced photoelectron spectra at photon energies above the electron affinity. The spectra were labeled with dn indicating an electronic excitation from the ground state of AuF^- to a DBS with a vibrational excitation to the nth vibrational state simultaneously. The spectra labeled with r are assigned to the resonant state related to 1 $^2\Pi_{3/2}$ of AuF^- tentatively. The energies of these excited states are higher than the electron affinity of AuF. Therefore, they quickly autodetached by ejecting an electron due to the vibronic coupling.[43] Since the extra electron was loosely bounded by the dipole potential, the potential curve of a DBS was almost parallel to that of its neutral core AuF. As a result, there was a propensity rule of the vibrational quantum change $\Delta n = -1$ during the autodetachment.[44–48] It can be seen that the intensity of the peak with a vibration quantum number equal to $n - 1$ was enhanced for each spectrum in Fig. 6 except the spectrum d3. For d3, both $n = 0$ and $n = 2$ were clearly enhanced, which was also reflected in the photoelectron angular distributions of $n = 0$ and $n = 2$. Both are isotropic. As shown in Fig. 1, the photoelectron angular distribution is parallel to the laser polarization for the direct photodetachment from the ground state $X^2\Sigma^+$. And, as shown in Fig. 6, it is isotropic for the autodetachment from a DBS. It should be noted that for $n = 0$, we have $\Delta n = -3$, which is very unusual for the autodetachment from a DBS. The propensity rule is derived based on harmonic approximation,[49] and violation of this rule has been observed previously due to anharmonic effects.[50–54] The violation of the propensity rule may also result from the non-negligible correlation effects between the DBS electron and other electrons.[55] The interaction between DBS and VES has been discussed in some molecules, such as nitromethane,[56,57] uracil,[58,59] nitrobenzene,[60] and thymine dimer.[61] Here, the interaction between DBS d3 and a VES may result in the violation of the propensity rule. It should be noted that the lifetimes of these excited states[43] should be much shorter

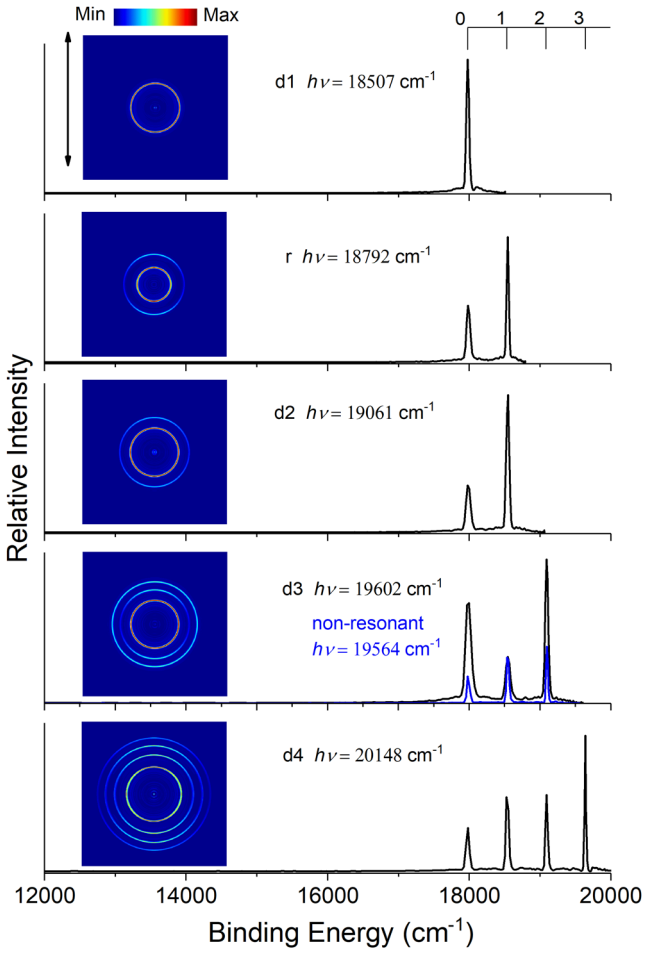

FIG. 6. Resonance-enhanced photoelectron spectra and images of AuF^- acquired using the OPO signal light. The labels d1 to d4 indicate the resonance via the DBS with vibrational quantum numbers equal to 1, 2, 3, and 4. For d3, the non-resonant photoelectron spectrum collected at a photon energy of 19 564 cm^{-1} is also shown in comparison. The label *r* indicates a resonance that is tentatively assigned to 1 $^2\Pi_{3/2}$. The vibrational quantum number of the final AuF ($X^1\Sigma^+$) state is marked on the top.

than the duration of the laser pulse (~5 ns) because no two-photon detachment was observed. As a contrast, the lifetime of excited states v0–v5 and d0 should be comparable with the duration of the laser pulse. Otherwise, they cannot be photodetached by a second photon before decaying.

IV. CONCLUSION

In conclusion, the resonant photodetachment spectra of cryogenically cooled AuF^- were obtained via the slow-electron velocity-map imaging (SEVI) method. The electron affinity of AuF was measured as 17 976(8) cm^{-1} or 2.2287(10) eV. Around the photodetachment threshold, a dipole-bound state with a binding energy 24(8) cm^{-1}, a valence excited state with a binding energy 1222(11) cm^{-1}, and a resonant state with an energy 814(12) cm^{-1} above the photodetachment threshold were observed. An unusual vibrational transition was observed in the vibrationally induced autodetachment from the dipole-bound state. Moreover, two excited states of neutral AuF were observed for the first time, located at 13 720(78) cm^{-1} and 16 188(44) cm^{-1} above the AuF ground state.

ACKNOWLEDGMENTS

This work was supported by the National Natural Science Foundation of China (NSFC) (Grant No. 11974199, 91736102) and the National Key R&D Program of China (Grant No. 2018YFA0306504).

DATA AVAILABILITY

The data that support the findings of this study are available from the corresponding author upon reasonable request.

REFERENCES

[1] F. Mohr, Gold Bulletin **37**, 164 (2004).
[2] D. Schröder *et al.*, Angew. Chem. **106**, 223 (1994).
[3] K. L. Saenger and C. P. Sun, Phys. Rev. A **46**, 670 (1992).
[4] E. K. Butler *et al.*, J. Phys. Chem. A **114**, 4831 (2010).
[5] T. C. Steimle *et al.*, J. Phys. Chem. A **117**, 11737 (2013).
[6] O. H. Crawford, Mol. Phys. **20**, 585 (1971).
[7] C. Desfrançois *et al.*, Phys. Rev. Lett. **73**, 2436 (1994).
[8] C. Desfrançois, H. Abdoul-Carime, and J.-P. Schermann, Int. J. Mod. Phys. B **10**, 1339 (1996).
[9] N. I. Hammer *et al.*, J. Chem. Phys. **119**, 3650 (2003).
[10] N. I. Hammer *et al.*, J. Chem. Phys. **120**, 685 (2004).
[11] C.-H. Qian, G.-Z. Zhu, and L.-S. Wang, J. Phys. Chem. Lett. **10**, 6472 (2019).
[12] P. Schwerdtfeger *et al.*, J. Chem. Phys. **91**, 1762 (1989).
[13] P. Schwerdtfeger *et al.*, Chem. Phys. Lett. **218**, 362 (1994).
[14] P. Schwerdtfeger *et al.*, J. Chem. Phys. **103**, 245 (1995).
[15] J. K. Laerdahl, T. Saue, and K. Faegri, Jr., Theor. Chem. Acc. **97**, 177 (1997).
[16] M. Iliaš, P. Furdík, and M. Urban, J. Phys. Chem. A **102**, 5263 (1998).
[17] C. van Wüllen, J. Chem. Phys. **109**, 392 (1998).
[18] W. Liu and C. van Wüllen, J. Chem. Phys. **110**, 3730 (1999).
[19] M. Guichemerre, G. Chambaud, and H. Stoll, Chem. Phys. **280**, 71 (2002).
[20] F. Wang and L. Li, Theor. Chem. Acc. **108**, 53 (2002).
[21] S. Andreev and J. J. BelBruno, Chem. Phys. Lett. **329**, 490 (2000).
[22] D. B. Dao and R. Mabbs, J. Chem. Phys. **141**, 154304 (2014).
[23] T.-C. Jagau *et al.*, J. Phys. Chem. Lett. **6**, 2786 (2015).
[24] A. Osterwalder *et al.*, J. Chem. Phys. **121**, 6317 (2004).
[25] D. M. Neumark, J. Phys. Chem. A **112**, 13287 (2008).
[26] I. León *et al.*, Rev. Sci. Instrum. **85**, 083106 (2014).
[27] Z.-H. Luo *et al.*, Phys. Rev. A **93**, 020501 (2016).
[28] M. L. Weichman and D. M. Neumark, Annu. Rev. Phys. Chem. **69**, 101 (2018).
[29] X.-L. Chen and C.-G. Ning, Phys. Rev. A **93**, 052508 (2016).
[30] R.-L. Tang, X.-X. Fu, and C.-G. Ning, J. Chem. Phys. **149**, 134304 (2018).
[31] C. Hock *et al.*, J. Chem. Phys. **137**, 244201 (2012).
[32] X.-B. Wang and L.-S. Wang, Rev. Sci. Instrum. **79**, 073108 (2008).
[33] W. C. Wiley and I. H. McLaren, Rev. Sci. Instrum. **26**, 1150 (1955).
[34] B. Dick, Phys. Chem. Chem. Phys. **21**, 19499 (2019).

[35]R.-L. Tang *et al.*, arXiv:1910.02188 (2019).
[36]H.-J. Werner *et al.*, Wiley Interdiscip. Rev.: Comput. Mol. Sci. **2**, 242 (2012).
[37]K. A. Peterson and C. Puzzarini, Theor. Chem. Acc. **114**, 283 (2005).
[38]R. A. Kendall, T. H. Dunning, Jr., and R. J. Harrison, J. Chem. Phys. **96**, 6796 (1992).
[39]W. Gordy and R. L. Cook, *Microwave Molecular Spectra* (Wiley, 1984).
[40]C. Blondel, C. Delsart, and F. Goldfarb, J. Phys. B: At., Mol. Opt. Phys. **34**, L281 (2001).
[41]T. Okabayashi *et al.*, Chem. Phys. Lett. **366**, 406 (2002).
[42]J. C. López V. *et al.*, Int. J. Quantum Chem. **88**, 280 (2002).
[43]D. H. Kang, S. An, and S. K. Kim, Phys. Rev. Lett. **125**, 093001 (2020).
[44]J. Simons, J. Am. Chem. Soc. **103**, 3971 (1981).
[45]P. K. Acharya, R. A. Kendall, and J. Simons, J. Am. Chem. Soc. **106**, 3402 (1984).
[46]D. M. Wetzel and J. I. Brauman, J. Chem. Phys. **90**, 68 (1989).
[47]H. T. Liu *et al.*, Angew. Chem., Int. Ed. **52**, 8976 (2013).
[48]H. T. Liu *et al.*, Angew. Chem., Int. Ed. **53**, 2464 (2014).
[49]R. S. Berry, J. Chem. Phys. **45**, 1228 (1966).
[50]D.-L. Huang *et al.*, Chem. Phys. **482**, 374 (2017).
[51]D.-L. Huang *et al.*, Chem. Sci. **6**, 3129 (2015).
[52]G.-Z. Zhu, D.-L. Huang, and L.-S. Wang, J. Chem. Phys. **147**, 013910 (2017).
[53]D.-L. Huang *et al.*, J. Mol. Spectrosc. **332**, 86 (2017).
[54]G.-Z. Zhu and L.-S. Wang, Chem. Sci. **10**, 9409 (2019).
[55]G.-Z. Zhu *et al.*, J. Phys. Chem. Lett. **10**, 4339 (2019).
[56]R. N. Compton *et al.*, J. Chem. Phys. **105**, 3472 (1996).
[57]T. Sommerfeld, Phys. Chem. Chem. Phys. **4**, 2511 (2002).
[58]C. Desfrançois *et al.*, J. Phys. Chem. A **102**, 1274 (1998).
[59]J. H. Hendricks *et al.*, J. Chem. Phys. **108**, 8 (1998).
[60]C. Desfrancois *et al.*, J. Chem. Phys. **111**, 4569 (1999).
[61]A. F. Jalbout, J. Smets, and L. Adamowicz, Chem. Phys. **273**, 51 (2001).